Strong Nonlinear Coupling in a Si_3N_4 Ring Resonator

Sven Ramelow,[1,*] Alessandro Farsi,[2,*] Zachary Vernon,[3] Stephane Clemmen,[4] Xingchen Ji,[5] J. E. Sipe,[3] Marco Liscidini,[6,†] Michal Lipson,[5] and Alexander L. Gaeta[2]

[1]*Institute for Physics, Humboldt University, 12489 Berlin, Germany*
[2]*Department of Applied Physics and Applied Math, Columbia University, New York 10027, New York, USA*
[3]*Department of Physics, University of Toronto, Toronto M5S 1A7, Canada*
[4]*Department of Information Technology, Ghent University, 9000 Ghent, Belgium*
[5]*Department of Electrical Engineering, Columbia University, New York 10027, New York, USA*
[6]*Dipartimento di Fisica, Università degli Studi di Pavia, 21700 Pavia, Italy*

(Received 19 December 2018; published 19 April 2019)

We demonstrate that nondegenerate four-wave mixing in a Si_3N_4 microring resonator can result in a nonlinear coupling rate between two optical fields exceeding their energy dissipation rate in the resonator, corresponding to strong nonlinear coupling. We demonstrate that this leads to a Rabi-like splitting, for which we provide a theoretical description in agreement with our experimental results. This yields new insight into the dynamics of nonlinear optical interactions in microresonators and access to novel phenomena.

DOI: 10.1103/PhysRevLett.122.153906

When two identical oscillators of frequency ω_0 are linearly coupled with a coupling rate Γ larger than the dissipation rate γ, their dynamics can be described in terms of two new supermodes with frequencies $\omega_0 - \Omega/2$ and $\omega_0 + \Omega/2$, where the splitting term Ω is known as the Rabi frequency. The two oscillators are said to be in the strong coupling regime. This often arises in physics, for a large variety of systems can be described in terms of coupled oscillators. Plasmon polaritons, which result from the strong coupling of the optical field with collective charge oscillations, are a familiar example [1].

Similar dynamics can occur in the strong coupling of two optical fields. Recently, this has been observed experimentally in frequency conversion via sum frequency generation in a AlN ring resonator [2] and via Bragg scattering in a Si_3N_4 ring resonator [3]. In both experiments, the coupling rate between the seed and up-converted fields could exceed the energy damping rate in the resonator, leading to a Rabi splitting of the seed and up-converted resonances. High-quality-factor microresonators were instrumental in both increasing the coupling between the two fields and maintaining the energy dissipation rate as small as possible. Although the coupling of the optical fields in these experiments was due to second- and third-order nonlinearities, respectively, and induced by a strong pump field with respect to the seed and up-converted fields, the coupling was linear, with the Rabi splitting being independent of the intensity of those two fields.

A qualitatively different situation was investigated by Carusotto and La Rocca [4], who suggested that Rabi-like splitting should also be observed in second harmonic generation in a doubly resonant cavity, when the coupling rate of the fundamental field at ω with the up-converted field at 2ω is larger than the energy dissipation rate in the cavity. In this scenario, since the coupling between the fields is quadratic in the amplitude of the optical field at ω, the magnitude of the splitting increases with the intensity of the fundamental field. Here, one has an example of strong nonlinear coupling where the adjective "nonlinear" refers to the quadratic dependence of the coupling on the amplitude of one of the fields. Later, the same idea was proposed at the quantum level, with the nonlinear coupling occurring between two photons at the fundamental mode at ω and one photon at 2ω in a doubly resonant photonic crystal cavity [5]. Despite these two promising theoretical proposals, the observation of this strong nonlinear coupling regime has yet to be demonstrated experimentally.

In this Letter, we show that strong nonlinear coupling can be observed in a Si_3N_4 ring resonator. Our approach was inspired by the work of Langford *et al.* [6], who argued that the use of a strong pump for one of the fields of a four-wave mixing (FWM) process in a $\chi^{(3)}$-nonlinear medium can lead to an effective $\chi^{(2)}$ nonlinearity for the remaining three fields. Not directly limited by the intrinsic material properties, this effective $\chi^{(2)}$ interaction can be made very large by increasing the pump power. To date, such an effective $\chi^{(2)}$ has been demonstrated at relatively low efficiencies using a photonic crystal fiber [6], a chalcogenide nanofiber [7], and a resonant $\chi^{(3)}$ nonlinearity in warm Rb vapor [8]. This approach is also compatible with material platforms and light confinement strategies characterized by strong field enhancements and exceptionally large quality factors (Q's), which offer the promise of strong effective second-order interactions. We shall show

below that this platform can give access to nonlinear phenomena that cannot be readily observed in a material with a natural $\chi^{(2)}$. While a description of the third-order nonlinear interaction in terms of an effective $\chi^{(2)}$ is not necessary to explain the experimental results, such a narrative can help identify phenomena in third-order nonlinear systems that are analogous to those in second-order nonlinear systems.

We consider the case in which a strong pump field stimulates the conversion of two seed photons [see Fig. 1(a)] to one photon at a higher energy and one photon at the pump frequency. We consider this process in a high-Q Si_3N_4 microresonator, which gives rise to dramatic enhancements of both the circulating pump power available and the nonlinear interaction between the three fields [9–13]. The Si_3N_4 material was chosen to avoid two-photon absorption and Raman scattering, which typically plague the performances of silicon and silica systems operating at high internal powers.

For the theoretical description we consider the resonant nonlinear interaction of the three fields as schematically indicated in Fig. 1(a). There is a strong pump at ω_P, a weak seed at ω_S, and an idler generated at $\omega_I = 2\omega_S - \omega_P$. We focus on the time-dependent effective second-order nonlinear interaction between the seed and the idler, which can be described by the equations

$$\frac{d\beta_S}{dt} = -\bar{\Gamma}_S\beta_S + 2i\Lambda_2(t)\beta_S^*\beta_I - i\gamma_S^*\alpha_S e^{-i\Delta_S t}, \quad (1)$$

$$\frac{d\beta_I}{dt} = -\bar{\Gamma}_I\beta_I + i\Lambda_2^*(t)\beta_S^2, \quad (2)$$

where $\beta_{S,I}$ are the slowly varying seed and idler field amplitudes in the resonator, $\bar{\Gamma}_{S,I}$ are the total resonator damping rates at $\omega_{S,I}$, α_S is the amplitude of the seed driving field in the bus waveguide, Δ_S is the detuning away from resonance, and γ_S characterizes the coupling between the bus waveguide and the ring. The coefficient $\Lambda_2(t)$, which describes the strength of the effective $\chi^{(2)}$, is given by $\Lambda_2(t) = \Lambda_3\beta_P(t)$, with $\Lambda_3 \approx \hbar\omega v_g^2\gamma_{\mathrm{NL}}/(2\pi R)$ the third-order coupling coefficient, where γ_{NL} is the usual nonlinear parameter, v_g the group velocity in the ring at ω_P, R the ring radius, and $\omega^2 = \sqrt{\omega_P\omega_S^2\omega_I}$; $\beta_P(t)$ is the pump amplitude in the ring. We assume that $\beta_P(t)$ is undepleted and that the effects of self- and cross-phase modulation are taken into account as corrections to the resonant frequencies $\omega_{S,I,P}$, which is valid for slowly varying field envelope functions; we restrict our analysis to this regime [14].

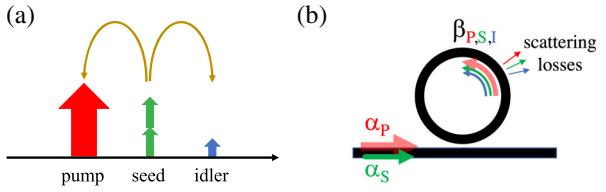

FIG. 1. FWM process driven by a strong field at ω_P (a) can be modeled as a time-dependent effective second-order nonlinear interaction leading to the generation of the idler field. (b). Sketch of the FWM process in a single-bus waveguide ring resonator (c).

The steady-state solutions of Eqs. (1) and (2) can be used to identify the occurrence of the strong nonlinear coupling regime, in which the nonlinear coupling rate $\Lambda_3|\beta_P\beta_S|$ between the modes exceeds the energy loss rate of the resonator. In particular, one should observe a splitting of the seed resonance when the "resolvability" R, i.e., the ratio of the splitting to the resonance linewidth, is nearly unity. This quantity depends on the ring parameters as well as on the pump and seed power, according to

$$R = \left|\frac{\Lambda_3\beta_S\beta_P}{\bar{\Gamma}_S}\right| \approx \frac{8\Lambda}{\omega_S}\sqrt{\frac{P_P P_S}{\hbar\omega_S^2\hbar\omega_P^2}}\frac{Q_P}{\sqrt{Q_P^{\mathrm{ext}}}}\frac{Q_S^2}{\sqrt{Q_S^{\mathrm{ext}}}}, \quad (3)$$

where $P_{P,S}$ are the pump and seed input powers and $Q_{P,S}^{\mathrm{ext}}$ are the extrinsic quality factors of the resonators determined solely by the external coupling. The last term of the equation is obtained by assuming a linear solution for the pump and the seed powers and is strictly valid for $R < 1$; it allows one to have a rough estimate of when the strong nonlinear coupling regime can be achieved.

The chip-integrated microring resonators utilized in this work were made from a high-quality Si_3N_4 film on an SiO_2 substrate, grown via low-pressure chemical vapor deposition and electron beam lithography (see Luke *et al.* [19] for details). The waveguide dimensions of 730 nm × 910 nm (height × width) are carefully chosen to achieve zero group velocity dispersion at 1410 nm, with the waveguide exhibiting phase matching between a strong pump at 1590 nm, the seed field at 1400 nm, and the idler field at 1260 nm. Moreover, the large normal group velocity dispersion at ω_P strongly inhibits any undesired parametric process from the strong pump (e.g., spontaneous degenerate FWM generating photons at ω_S and $2\omega_P - \omega_S$). The microresonator (radius 45 μm) with a free spectral range of 500 GHz is coupled to the bus waveguide with a gap of 450 nm and exhibits loaded Q factors of 250 000 for the pump (overcoupled), 1.2×10^6 for the seed (close to critical coupling), and about 3.5×10^6 for the idler (undercoupled).

The experimental configuration is shown in Fig. 2. The continuous wave pump and seed light are generated by tunable external cavity lasers. The pump is amplified with a high-power erbium doped fiber amplifier and combined with the seed by means of wavelength division multiplexers (WDMs). They are injected into the chip (and collected) via lensed fibers with a total insertion loss of 8.5 dB, resulting in 85 mW of on-chip pump power at 1590 nm. The output is separated into the three wavelength bands by cascaded WDMs to be monitored separately on InGaAs photodiodes.

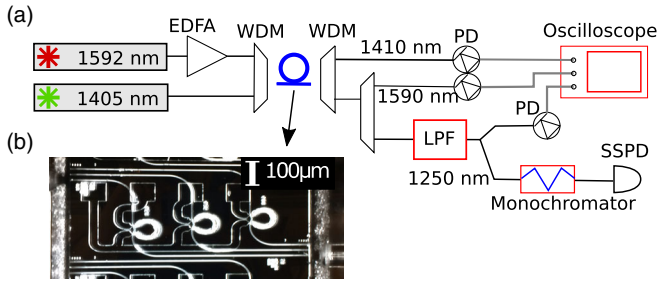

FIG. 2. (a) Schematics of the experiment. EDFA, erbium doped fiber amplifier; WDM, wave division multiplexing; LPF, low-pass filter; PD photodiode, SSPD superconducting single-photon detectors. The centers of the WDM channel and threshold of the LPF are 1592, 1405, and 1250 nm, respectively. (b) Microscope image of part of the microresonator chip. The sample detail shows three different resonators, and the lensed fiber for input-output coupling on the right side of the chip.

The idler output at 1260 nm is further strongly filtered by a low-pass filter, yielding total losses of 6.3 dB, including the WDMs. When measuring very low intensities, we optionally filter the idler with a grating monochromator (0.55-nm filter bandwidth) and then detect it with superconducting single-photon detectors. We enclose the chip and stabilize the temperature to reduce thermal and mechanical effects.

We first measure the idler output power generated at 1260 nm as a function of power of the seed, which is tuned to 1400 nm. During the measurement the 1590-nm pump wavelength is tuned into resonance from the short wavelength side to follow the resonance thermal redshift and achieve thermal locking [20]. We start by setting the seed power in the bus waveguide to 350 μW and successively reduce it to nanowatt level. This allows us to study the system with the seed power ranging over 4 orders of magnitude.

The conversion efficiency, defined as the on-chip idler power divided by the on-chip seed power, is shown in Fig. 3. As expected, at low seed powers the effective conversion efficiency shows a linear dependence on seed power as indicated by the slope of the curve in the figure inset, in which data are shown on a log-log scale. In this regime, we can infer an on-chip seed nonlinear efficacy $P_{\mathrm{idler}}/P_{\mathrm{seed}}^2 = 74000\%/\mathrm{W}$, in excellent agreement with the theoretically predicted value of $87000 \pm 17000\%/\mathrm{W}$; the error interval is estimated from the uncertainty on the experimental parameters (e.g., coupled power, quality factors, and propagation losses). Since the conversion efficiency and the seed nonlinear efficacy depend on the pump power at 1590 nm, a comparison with traditional second-order nonlinear systems should be done with care.

At large seed powers of a few hundreds of microwatts, the conversion efficiency begin to saturate at 5%, which suggests that the nonlinear coupling of the modes can no longer be treated perturbatively, and we enter the regime of strong nonlinear coupling. We investigate this regime by

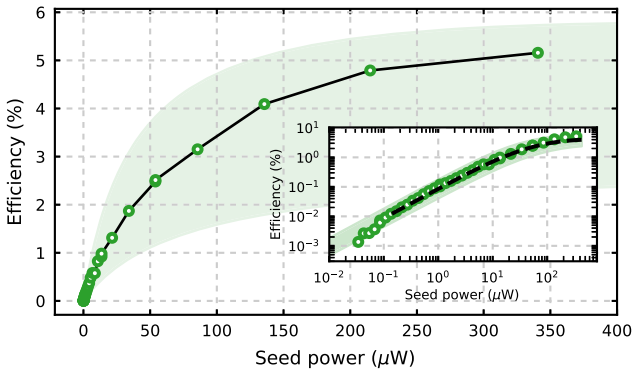

FIG. 3. Idler generation as a function of seed power. The main plot shows the inferred on-chip conversion efficiency as a function of seed power. The inset shows a double-logarithmic plot of the idler power vs seed power, where the dashed line is a trend curve that highlights the linear scaling between seed powers of about 0.1 μW, where the idler power arises above noise, to seed powers of about 10 μW, where saturation effects begin to be important. The shaded region indicates the theoretical expected trend within the estimated errors.

performing a second type of measurement to verify the presence of resonance splittings, which are the typical signature of the strong coupling regime. We scan the seed laser across the resonance wavelengths while the generated idler and seed transmitted powers are monitored. Typical scans are shown in Fig. 4 for seed power $P_{\mathrm{seed}} = 20$ μW (left) and $P_{\mathrm{seed}} = 300$ μW (right). At first sight, the presence of a broad peak at $P_{\mathrm{seed}} = 20$ μW could be confused with resonance splitting due to backscattering typical of some resonances in high-Q resonators. However, a gradual broadening of the seed peak can be observed as the seed power is increased, until two dips can be clearly resolved in the seed transmission spectra. Such splitting arises from the coupling term appearing in Eq. (2), which is

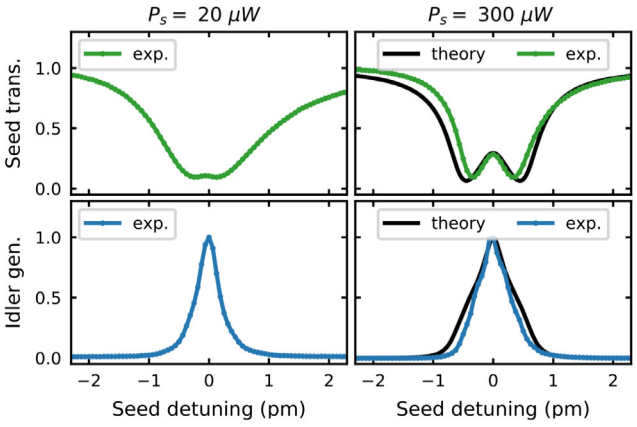

FIG. 4. Seed (green) transmission and idler (blue) generation when seed wavelength is scanned across the resonance. On the left, the seed power $P_{\mathrm{seed}} = 20$ μW. On the right, where $P_{\mathrm{seed}} = 300$ μW, the profiles are modified by the strong nonlinear coupling.

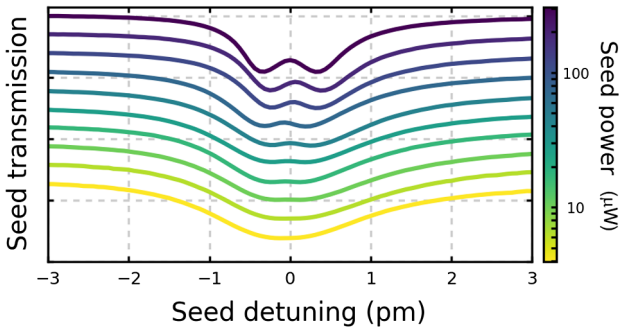

FIG. 5. Seed transmission as the seed wavelength is scanned across the seed resonance for different seed input power levels. A characteristic change of the resonance shape appears for higher seed power.

quadratic in the seed amplitude. The measurements are in very good agreement with the theoretical curves following from Eqs. (1) and (2) (see Supplemental Material [14]), in which we use the nominal parameters of the system without the need for any fitting.

Finally, in Fig. 5 we plot the seed transmission as a function of resonance detuning for several seed powers. Unlike previous studies in which Rabi oscillations are predicted [21] and Rabi splittings have been experimentally observed [2,3], the splitting magnitude here depends on the intensity of the seed field and not only on the pump power (with no observable splitting for seed powers below 10 μW), demonstrating the observation of strong nonlinear coupling.

In conclusion, we have shown that nondegenerate four-wave mixing in a microring resonator can be used to obtain nonlinear frequency conversion in a configuration that can be described in terms of a time-dependent second-order nonlinear coupling between two resonant fields. The use of Si_3N_4 microrings allows driving pump powers of hundreds of milliwatts in high-Q resonators without the limitation of two-photon absorption. This yields a measured seed nonlinear efficacy of 74000%/W for a few nanowatts seed powers, allowing the strong nonlinear coupling regime to be achieved with seed powers as low as a few microwatts. The experimental outcomes are in excellent agreement with our theoretical model. The peculiar features of nonlinear strong coupling, in which the system transmission is a function of the intensity of the input field, even at microwatt power levels, makes it extremely appealing in view of developing intensity-dependent solutions for photon switching and routing. At the same time, the continuous improvement of the quality factor of integrated microresonators suggests that strong nonlinear coupling might be found in other kinds of resonators and for different nonlinear interactions. Thus, while these results show among the highest conversion efficiency ever reported in an integrated device and confirm the maturity of the Si_3N_4 platform for coherent frequency conversion, they also give first evidence of a hitherto unexplored regime in nonlinear optical interactions that is worthy of further investigation from both applied and fundamental points of view.

*This author contributed equally to this work.
†Corresponding author.
marco.liscidini@unipv.it

[1] G. Grosso and G. Pastori Parravicini, *Solid State Physics*, 2nd ed. (Academic Press, London, 2014).
[2] X. Guo, C.-L. Zou, H. Jung, and H. X. Tang, On-Chip Strong Coupling and Efficient Frequency Conversion between Telecom and Visible Optical Modes, Phys. Rev. Lett. **117**, 123902 (2016).
[3] Q. Li, M. Davanço, and K. Srinivasan, Efficient and low-noise single-photon-level frequency conversion interfaces using silicon nanophotonics, Nat. Photonics **10**, 406 (2016).
[4] I. Carusotto and G. C. La Rocca, Two-photon Rabi splitting and optical Stark effect in semiconductor microcavities, Phys. Rev. B **60**, 4907 (1999).
[5] W. T. M. Irvine, K. Hennessy, and D. Bouwmeester, Strong Coupling between Single Photons in Semiconductor Microcavities, Phys. Rev. Lett. **96**, 057405 (2006).
[6] N. K. Langford, S. Ramelow, R. Prevedel, W. J. Munro, G. J. Milburn, and A. Zeilinger, Efficient quantum computing using coherent photon conversion, Nature (London) **478**, 360 (2011).
[7] E. Meyer-Scott, A. Dot, R. Ahmad, L. Li, M. Rochette, and T. Jennewein, Power-efficient production of photon pairs in a tapered chalcogenide microwire, Appl. Phys. Lett. **106**, 081111 (2015).
[8] P. Donvalkar, C. Joshi, S. Ramelow, and A. L. Gaeta, Quantum correlated photon-pairs from warm Rb-vapor, in *Proceedings of the Conference on Lasers and Electro-Optics, 2016* (Optical Society of America, Washington, DC, 2016), paper FTu1C.7.
[9] W. Bogaerts, P. De Heyn, T. Van Vaerenbergh, K. De Vos, K. S. Selvaraja, T. Claes, P. Dumon, P. Bienstman, D. Van Thourhout, and R. Baets, Silicon microring resonators, Lasers Photonics Rev. **6**, 47 (2012).
[10] A. C. Turner, M. A. Foster, A. L. Gaeta, and M. Lipson, Ultra-low power parametric frequency conversion in a silicon microring resonator, Opt. Express **16**, 4881 (2008).
[11] M. Ferrera, D. Duchesne, L. Razzari, M. Peccianti, R. Morandotti, P. Cheben, S. Janz, D.-X. Xu, B. E. Little, S. Chu, and D. J. Moss, Low power four wave mixing in an integrated, micro-ring resonator with $Q = 1.2$ million, Opt. Express **17**, 14098 (2009).
[12] A. Gondarenko, A. L. Gaeta, A. C. Turner-Foster, J. S. Levy, M. A. Foster, and M. Lipson, CMOS-compatible multiple-wavelength oscillator for on-chip optical interconnects, Nat. Photonics **4**, 37 (2010).
[13] X. Ji, F. A. S. Barbosa, S. P. Roberts, A. Dutt, J. Cardenas, Y. Okawachi, A. Bryant, A. L. Gaeta, and M. Lipson, Ultra-low-loss on-chip resonators with sub-milliwatt parametric oscillation threshold, Optica **4**, 619 (2017).
[14] See Supplemental Material at http://link.aps.org/supplemental/10.1103/PhysRevLett.122.153906, which includes Refs. [15–18], for more details on the theoretical description of the system dynamics.

[15] Z. Vernon and J. E. Sipe, Spontaneous four-wave mixing in lossy microring resonators, Phys. Rev. A **91**, 053802 (2015).

[16] Z. Vernon and J. E. Sipe, Strongly driven nonlinear quantum optics in microring resonators, Phys. Rev. A **92**, 033840 (2015).

[17] C. W. Gardiner and M. J. Collett, Input and output in damped quantum systems: Quantum stochastic differential equations and the master equation, Phys. Rev. A **31**, 3761 (1985).

[18] C. Wang, M. J. Burek, Z. Lin, H. A. Atikian, V. Venkataraman, I.-C. Huang, P. Stark, and M. Lončar, Integrated high quality factor lithium niobate microdisk resonators, Opt. Express **22**, 30924 (2014).

[19] K. Luke, A. Dutt, C. B. Poitras, and M. Lipson, Overcoming SiN film stress limitations for high quality factor ring resonators, Opt. Express **21**, 22829 (2013).

[20] T. Carmon, L. Yang, and K. J. Vahala, Dynamical thermal behavior and thermal self-stability of micro-cavities, Opt. Express **12**, 4742 (2004).

[21] Z. Vernon, M. Liscidini, and J. E. Sipe, Quantum frequency conversion and strong coupling of photonic modes using four-wave mixing in integrated microresonators, Phys. Rev. A **94**, 023810 (2016).